Modeling and Control of a Double Inverted Pendulum using LQR with Parameter Optimization through GA and PSO

Maki K. Habib and Samuel A. Ayankoso
The American University in Cairo
Cairo, Egypt
maki@aucegypt.edu and samuel_ayankoso@aucegypt.edu

***Abstract*—An inverted pendulum system has potential applications in different domains that motivate researchers for new innovative development. An inverted pendulum system is an underactuated, nonlinear, inherently unstable and a multivariable system. The system is modelled mainly through either Euler-Lagrange or Newtonian dynamic formulation. This paper aims to examine the control of a double inverted pendulum (DIP) using pole placement and linear quadratic regulator (LQR) control. To find the optimal parameters of the LQR control law, Genetic Algorithm (GA) and Particle Swarm Optimization (PSO) are used to tune and determine the proper control parameters. Simulations are conducted using MATLAB/Simulink under different circumstances and the performance of each control technique is analyzed and compared in terms of the system rise time, settling time, peak amplitude, and steady state error.**

Keywords— Double Inverted Pendulum, Underactuated, Unstable, Euler-Lagrange dynamic, Newtonian dynamic, Modern control, State feedback, LQR, Optimization, GA, PSO.

I. INTRODUCTION

An inverted pendulum system has a wide range of applications; its operational principle is used in rocket and missiles launch, segway design, humanoid locomotion design, pendubot design, investigation of human balancing, etc. [1], [2]. The inverted pendulum system is a practical example of a nonlinear, unstable, multivariable, and underactuated system which can be modeled and controlled in state space domain [1], [3]. The dynamics of this system is formulated mainly either through Euler-Lagrange dynamic formulation [1], [4], [5] or Newtonian dynamic formulation [3]. The resulting dynamic formulation, however, is nonlinear but can be linearized around any of the system equilibrium points – particularly the stable upright position. Then, the system linearized equations are used for state space representation.

Different control methods are applied to the linearized equations of single and double inverted pendulum systems, these include: proportional- integral-derivative (PID) control, pole placement control, linear quadratic regulator (LQR) control, fuzzy control, model predictive control (MPC), sliding mode control (SMC), etc. [6]–[11]. Some of these control techniques are combined to form a hybrid control technique such as PID+LQR and Fuzzy SMC [12], [13].

LQR was applied to a double inverted pendulum in [10] and [14], and the simulation results showed an improved performance in the settling time and peak amplitude of the two pendulums when the Q and R control parameters were tuned manually in [10]. The design and development of a mobile double inverted pendulum was presented in [11] and the performance of the system with LQR controller was evaluated through both simulation and experiment. In defining the Q matrix, more weight was given to the position states (and less weight for the velocity states) to control the pendulums and the cart quickly; the input weighting matrix (R) was defined in a way to have an input that match the limit of the driving DC motor: Q as diag(5000 5000 5000 5 5 5) and R as [1.0].

In [15], pole-placement technique was used to control an inverted pendulum on a cart. From the obtained results, the pendulum and the cart settled very fast when the two other poles used in the design of the control gain (aside the two dominant poles) get more negative. A separation factor of 2 was chosen in [16] between the dominant poles and the other poles, and this yielded a good performance. In addition, the performance of an inverted pendulum system with LQR and pole-placement techniques was investigated in [17] and the transient results of the pendulum and the cart with LQR indicated a better result as compared to the pole-placement control. The comparative advantage of LQR over PID was also investigated for a double inverted pendulum in [5] but a detailed analysis of LQR was not presented.

Furthermore, the stabilization of a rotary inverted pendulum was verified experimentally with double-PID+LQR and LQR in [12]. The double-PID+LQR controller improved the stabilization performance of the pendulum and its settling time by 83.33% and 62.5% respectively as compared to the LQR controller. In [18], a two-wheel inverted pendulum robot (TWIPR) was designed and controlled using fuzzy sliding mode control (FSMC) while a hybrid fuzzy adaptive controller was applied to an inverted pendulum in [13] which performed better than PID and LQR.

Moreover, many optimization methods like particle swarm optimization (PSO), genetic algorithm (GA) and bees algorithm (BA) are used to optimize the parameters of the controllers designed for an inverted pendulum system [19]–[21]. In [22], a GA-tuned PID controller gave a faster and better response compared to traditional PID controller for an inverted pendulum. The traditional PID is tuned by Ziegler-Nichols method, or sometimes by trial-and-error procedure which leads to non-optimal gains. The optimal tuning of a LQR controller for an inverted pendulum using BA was investigated in [23] while PSO was used in [24].

This paper presents the performance analysis and comparison of a linearized double inverted pendulum system with two different control techniques (pole placement and LQR methods) through simulation in MATLAB/Simulink. In

978-1-7281-6224-9/20/$31.00 ©2020 IEEE

2020 21st International Conference on Research and Education in Mechatronics (REM) | 978-1-7281-6224-9/20/$31.00 ©2020 IEEE | DOI: 10.1109/REM49740.2020.9313893

addition, GA and PSO are used to tune the Q and R matrices needed in the design of an LQR controller.

II. SYSTEM MODELING

This section presents the schematic of a planar DIP system and the non-linear mathematical model in part A, while part B and C deal with the linearization of the non-linear mathematical model and the state space representation, respectively.

A. The Physical and Mathematical Model of a DIP on a Cart

Euler-Lagrange dynamic formulation is used to model DIP in [4], [5]. This section introduces the derivation of the nonlinear dynamic equation of DIP based on the principles of Euler-Lagrange approach. The physical model of the system is illustrated in Fig. 1 and its parameters are described in Table I.

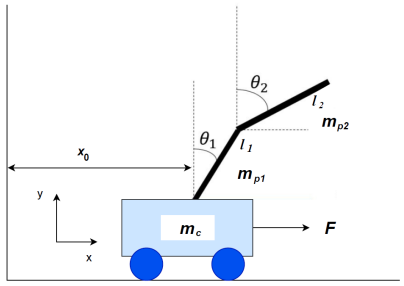

Fig. 1. A Double Inverted Pendulum (DIP) on a cart

Table I. Parameters of a double inverted pendulum

Parameter	Value	Unit
Mass of the cart, m_c	0.7	Kg
Mass of the lower pendulum, m_{p1}	0.5	Kg
Mass of the upper pendulum, m_{p2}	0.3	Kg
Earth's gravity, g	9.8	m/s^2
Length of the lower pendulum, l_1	0.45	m
Length of the upper pendulum, l_2	0.35	m
Moment of inertia of the lower pendulum, J_1	0.005	kg.m^2
Moment of inertia of the upper pendulum, J_2	0.005	kg.m^2

Euler-Lagrange dynamic formulation is expressed as

$$\frac{\partial}{\partial t}\left(\frac{\partial L}{\partial \dot{q}_i}\right)-\left(\frac{\partial L}{\partial q_i}\right)=F_i \tag{1}$$

From Euler-Lagrange equation, F_i represent the generalized system forces or external inputs, q_i is representing the system coordinates and L is called the Lagrangian and it is the difference between the total kinetic (T) and the total potential (P) energy in the system.

$$L=T-P \tag{2}$$

Where

$$T = T_0 + T_1 + T_2 \tag{3}$$

Where T_0, T_1, T_2 are the kinetic energy terms for the cart, the lower pendulum, and the upper pendulum, respectively.

$$\mathrm{T}_0=\frac{1}{2}m_c\dot{x}_0^2 \tag{4}$$

$$T_1 = \frac{1}{2}m_{p1}[\dot{x}_0 + \dot{\theta}_1 l_1 \cos\theta_1]^2 + \frac{1}{2}m_{p1}\dot{\theta}_1^2 l_1^2 \sin^2\theta_1 + \frac{1}{2}J_1\dot{\theta}_1^2 \tag{5}$$

$$\mathrm{T}_2=\frac{1}{2}m_{p2}[\dot{x}_0+\dot{\theta}_1 l_1\cos\theta_1+\dot{\theta}_2 l_2\cos\theta_2]^2+\frac{1}{2}m_{p2}[\dot{\theta}_1 l_1\sin\theta_1+\dot{\theta}_2 l_2\sin\theta_2]^2+\frac{1}{2}J_1\dot{\theta}_2^2 \tag{6}$$

Where x_0 is the cart position; θ_1 is the lower pendulum angle and θ_2 is the upper pendulum angle

Then, T can be obtained as

$$\mathrm{T}=\frac{1}{2}(m_c+m_{p1}+m_{p2})\dot{x}_0^2+\frac{1}{2}(m_{p1}l_1^2+m_{p2}l_1^2+J_1)\dot{\theta}_1^2+\frac{1}{2}(m_{p2}l_2^2+J_2)\dot{\theta}_2^2+(m_{p1}l_1+m_{p2}l_1)\dot{x}_0\dot{\theta}_1\cos\theta_1+m_{p2}l_2\dot{x}_0\dot{\theta}_2\cos\theta_2+m_{p2}l_1l_2\cos(\theta_1-\theta_2)\dot{\theta}_1\dot{\theta}_2 \tag{7}$$

The total potential energy in the system is:

$$P = P_0 + P_1 + P_2 \tag{8}$$

Where P_0, P_1, P_2 are the potential energy terms for the cart, the lower pendulum, and the upper pendulum, respectively.

$$P_0=0 \tag{9}$$

$$P_1 = m_{p1}gl_1\cos\theta_1 \tag{10}$$

$$P_2 = m_{p2}g(l_1\cos\theta_1+l_2\cos\theta_2) \tag{11}$$

Then, the total potential energy is:

$$P=(m_{p1}l_1+m_{p2}l_1)g\cos\theta_1+m_{p2}gl_2\cos\theta_2 \tag{12}$$

Accordingly, L can be obtained as

$$L=\frac{1}{2}(m_c+m_{p1}+m_{p2})\dot{x}_0^2+\frac{1}{2}(m_{p1}l_1^2+m_{p2}l_1^2+J_1)\dot{\theta}_1^2+\frac{1}{2}(m_{p2}l_2^2+J_2)\dot{\theta}_2^2+(m_{p1}l_1+m_{p2}l_1)\dot{x}_0\dot{\theta}_1\cos\theta_1+m_{p2}l_2\dot{x}_0\dot{\theta}_2\cos\theta_2+m_{p2}l_1l_2\cos(\theta_1-\theta_2)\dot{\theta}_1\dot{\theta}_2-(m_{P1}l_1+m_{P2}l_1)g\cos\theta_1-m_{P2}gl_2\cos\theta_2 \tag{13}$$

Let q_i represent the system variables in (13): x_0 , θ_1 and θ_2 Then, three equations of motions are developed using (1). The Lagrange equation with x_0 component has an external input denoted by u .

$$(m_c + m_{p1} + m_{p2})\ddot{x}_0 + (m_{p1}l_1 + m_{p2}l_1)\ddot{\theta}_1 \cos\theta_1 + m_{p2}l_2\ddot{\theta}_2 \cos\theta_2 - (m_{p1}l_1 + m_{p2}l_1)\dot{\theta}_1^2 \sin\theta_1 - m_{p2}l_2\dot{\theta}_2^2 \sin\theta_2 = u \quad (14)$$

$$(m_{p1}l_1^2 + m_{p2}l_1^2 + J_1)\ddot{\theta}_1 + (m_{p1}l_1 + m_{p2}l_1)\ddot{x}_0 \cos\theta_1 + m_{p2}l_1l_2 \cos(\theta_2 - \theta_1)\ddot{\theta}_2 + m_{p2}l_1l_2 \sin(\theta_2 - \theta_1)\dot{\theta}_1^2 - (m_{p1}l_1 + m_{p2}l_1)g \sin\theta_1 = 0 \quad (15)$$

$$(m_{p2}l_2^2 + J_2)\ddot{\theta}_2 + m_{p2}l_2\ddot{x}_0 \cos\theta_2 + m_{p2}l_1l_2 \cos(\theta_1 - \theta_2)\ddot{\theta}_1 + m_{p2}l_1l_2 \sin(\theta_1 - \theta_2)\dot{\theta}_1^2 - m_{p2}l_2 g \sin\theta_2 = 0 \quad (16)$$

B. Linearization of DIP

Equation (14), (15) and (16) are linearized about the pendulum upright position (at $\theta_1 = 0$ and $\theta_2 = 0$).

$$\cos\theta_1 = 1, \sin\theta_1 = \theta_1, \cos\theta_2 = 1, \sin\theta_2 = \theta_2$$
$$\cos(\theta_1 - \theta_2) = 1, \sin(\theta_1 - \theta_2) = \theta_1 - \theta_2$$
$$\dot{\theta}_1^2 = 0, \dot{\theta}_2^2 = 0, \dot{\theta}_1 = 0, \dot{\theta}_2 = 0$$

This yields three linear equations

$$a_0\ddot{x}_0 + a_1\ddot{\theta}_1 + a_3\ddot{\theta}_2 = u \quad (17)$$

$$a_1\ddot{x}_0 + a_2\ddot{\theta}_1 + a_4\ddot{\theta}_2 - a_1 g\theta_1 = 0 \quad (18)$$

$$a_3\ddot{x}_0 + a_4\ddot{\theta}_1 + a_5\ddot{\theta}_2 - a_3 g\theta_2 = 0 \quad (19)$$

Where

$$a_0 = m_c + m_{p1} + m_{p2}\ ;\ a_1 = (m_{p1} + m_{p2})l_1;$$
$$a_2 = m_{p1}l_1^2 + m_{p2}l_1^2 + J_1\ ;\ a_3 = m_{p2}l_2;$$
$$a_4 = m_{p2}l_1l_2\ ;\ a_5 = m_{p2}l_2^2 + J_2$$

C. State Space Representation of DIP

Equation (17), (18) and (19) can be expressed using state space representation as

$$x_1 = x_0;\ x_2 = \dot{x}_0;\ x_3 = \theta_1;\ x_4 = \dot{\theta}_1;\ x_5 = \theta_2;\ x_6 = \dot{\theta}_2$$

$$\dot{x}_1 = x_2 \quad (20)$$

$$\dot{x}_2 = px_3 + qx_5 + ku \quad (21)$$

$$\dot{x}_3 = x_4 \quad (22)$$

$$\dot{x}_4 = rx_3 + vx_5 + wu \quad (23)$$

$$\dot{x}_5 = x_6 \quad (24)$$

$$\dot{x}_6 = ex_3 + zx_5 + nu \quad (25)$$

Where

$$q = \left(\frac{-a_3 z}{a_0} - \frac{a_1 v}{a_0}\right); p = \left(\frac{-a_3 e}{a_0} - \frac{a_1 r}{a_0}\right); k = \left(\frac{1}{a_0} - \frac{a_3 n}{a_0} - \frac{a_1 w}{a_0}\right)$$

$$n = \frac{-b_1}{b_2}; z = \frac{-b_4 b_5 a_3 g}{b_2}; e = \frac{b_1 b_3 (a_1 g) + b_5 (a_1 g)}{b_2}$$

$$r = \left(\frac{b_3 a_1 g}{b_5} - \frac{b_6 (b_1 b_3 (a_1 g) + b_5 (a_1 g))}{b_2 b_5}\right)$$

$$w = \left(\frac{-1}{b_5} - \frac{b_6 b_1}{b_5 b_2}\right); v = \left(\frac{-b_6 b_4 a_3 g}{b_2}\right);\ b_1 = \left(\frac{a_4 a_1}{a_3} - a_2\right);$$

$$b_2 = \left(a_4 - \frac{a_1 a_5}{a_3}\right)\left(\frac{a_2 a_0}{a_1} - a_1\right) - \left(\frac{a_4 a_1}{a_3} - a_2\right)\left(a_3 - \frac{a_4 a_0}{a_1}\right)$$

$$b_3 = \left(\frac{a_0}{a_1}\right); b_4 = \left(\frac{a_1}{a_3}\right); b_5 = \left(\frac{a_2 a_0}{a_1} - a_1\right); b_6 = \left(a_3 - \frac{a_4 a_0}{a_1}\right)$$

$$\begin{bmatrix} \dot{x}_1 \\ \dot{x}_2 \\ \dot{x}_3 \\ \dot{x}_4 \\ \dot{x}_5 \\ \dot{x}_6 \end{bmatrix} = \begin{bmatrix} 0 & 1 & 0 & 0 & 0 & 0 \\ 0 & 0 & p & 0 & q & 0 \\ 0 & 0 & 1 & 0 & 0 & 1 \\ 0 & 0 & r & 0 & v & 0 \\ 0 & 0 & 0 & 0 & 0 & 1 \\ 0 & 0 & e & 0 & z & 0 \end{bmatrix} \begin{bmatrix} x_1 \\ x_2 \\ x_3 \\ x_4 \\ x_5 \\ x_6 \end{bmatrix} + \begin{bmatrix} 0 \\ k \\ 0 \\ w \\ 0 \\ n \end{bmatrix} u \quad (26)$$

$$y = Cx + Du \quad (27)$$

The matrix A, B, C, D of the system's dynamic equation are:

$$A = \begin{bmatrix} 0 & 1 & 0 & 1 & 0 & 0 \\ 0 & 0 & -10.3575 & 0 & -0.1575 & 0 \\ 0 & 0 & 1 & 0 & 0 & 1 \\ 0 & 0 & 53.0796 & 0 & -9.9235 & 0 \\ 0 & 0 & 0 & 0 & 0 & 0 \\ 0 & 0 & -34.0234 & 0 & 36.2736 & 0 \end{bmatrix} B = \begin{bmatrix} 0 \\ 1.3820 \\ 0 \\ -2.9358 \\ 0 \\ -0.1531 \end{bmatrix}$$

$$C = I_6;\quad D = [0]$$

Where I_6 is a 6 by 6 identity matrix

III. CONTROL DESIGN

In the section, part A shows the control design requirements and goals. This is followed by the discussion of pole placement control design in part B, LQR control design in part C and the tuning of LQR control with GA and PSO in part D.

A. Control Design Requirements and Goals

The design requirements in Table II were considered.

Table II. The desired control requirements for the DIP system

Pendulums	Requirement	Cart	Requirement
Settling time (s)	<3	Settling time	<3
Overshoot (deg.)	Max. 20	Rise time	0.5
Steady state error	0	Steady state error	0

The control goals are:

i. To stabilize the lower and upper pendulum at upright position, and

ii. To command the cart to a new position (0.1 meters).

The initial condition used for the purpose of simulation is:

x_0= [0; 0; 5*pi/180; 0; 5*pi/180; 0]

B. Pole Placement Control

In pole-placement method, the closed-loop poles are located at desired positions by means of a state feedback (with an appropriate gain for the system states). However, a necessary condition for placing a pole at any arbitrary point is that the system must be completely state controllable. This test is also known as the Kalman's test.

The system was tested for controllability, and a dominant pole placement of 4.6% overshoot and 1sec settling time was designed. Then, a separation factor of 2 was used for the other poles.

C. LQR Control

LQR is an optimal control technique that accounts for Q and R matrices representing the weights or cost functions to states deviation and control input respectively [11].

In (28), a function J_lqr (the performance index) is defined which can also be interpreted as the energy function. The objective in LQR design is to arrive at an optimal control law that minimizes the performance index [10].

$$J\_lqr = \frac{1}{2}\int_0^\infty (x^T Q x + u^T R u)dt \qquad (28)$$

Optimal control law: $u(t) = -Kx(t)$ (29)

Where u is the input of the control and K is the gain.

But a major concern in LQR design is the choice of the Q and R matrices.

Fig. 2 shows the block structure applicable for both pole-placement and LQR controller.

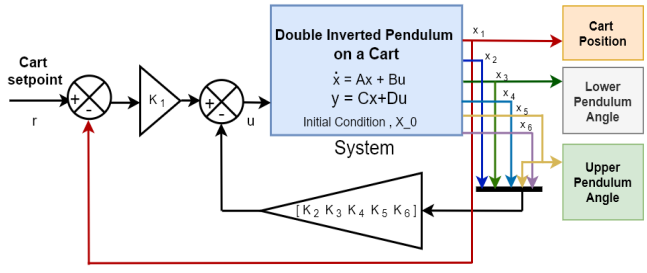

Fig. 2. The block diagram for pole-placement / LQR controller

D. Optimal Tuning of an LQR Controller with GA and PSO

Deciding the state and control weighing matrices (Q and R) that give the optimal control is time consuming by manual tuning; thus, an automatic tuning approach using Genetic Algorithm (GA) and Particle Swarm Optimization (PSO) are proposed separately for this purpose [21].

The first step when using GA or PSO to tune the Q and R matrices is to initialize the chromosome (genes) in the case of GA or the swarm particle in the case of PSO. Each chromosome or particle is represented by a vector z whose elements represent the Q and R matrices. Where z(1) represents Q(1,1), z(2) represents Q(3,3), z(3) represents Q(5,5) and z(4) represents R value. Then, other parameters like the population and bounds of the algorithms are also defined. To get the optimal control parameters, an objective function (J_optim) is proposed based on the control input and Integral Time Square Error (ITSE) [25].

$$J\_optim = \frac{1}{2}\int_0^\infty u^T R u \; dt + \int_0^\infty t.e^2 dt \qquad (30)$$

Both algorithms minimize this objective function through dissimilar processes as illustrated in Fig. 3 and the optimal solution is iteratively searched until the algorithm reached any of the stopping criteria such as the number of generations or iterations, function tolerance and time limit.

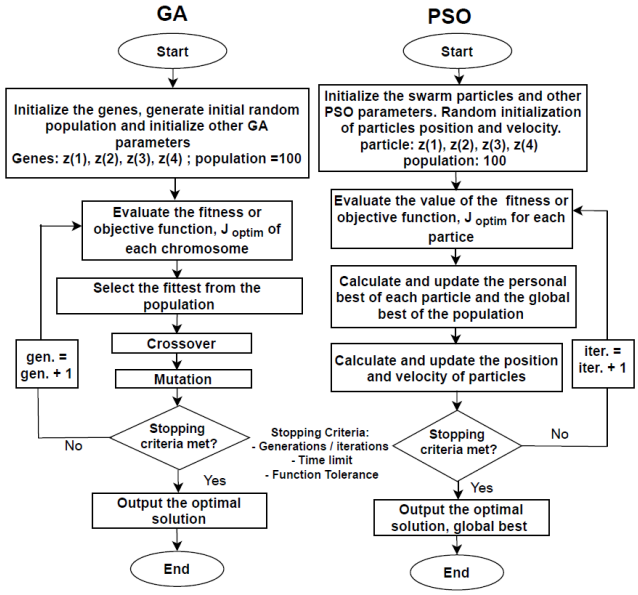

Fig. 3. Flowchart of GA and PSO LQR tuning

Fig. 4 shows the block diagram for a GA or PSO LQR tuning.

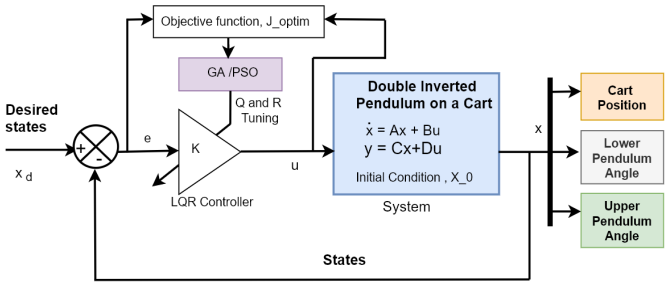

Fig. 4. The block diagram for GA/ PSO LQR (Q and R parameters) tuning

IV. SIMULATION

This section discusses the results of pole placement control, manual LQR control, GA and PSO tuned LQR control in Part A, B and C while the 2D animation of the system is captured in part D.

A. Simulation Results for Pole Placement Control

Based on the formulated requirements in Table I and the discussion in part B of section III, the desired pole location is: desired_pole = [-4+4.08j, -4-4.08j, -8, -8, -8, -8]

The controller gain, K is then calculated using this command: $K_{pole\text{-}placment}$ = acker (A, B,des_pole)

The obtained control gain was used with the system block diagram developed in Simulink (as illustrated in Fig. 2) and the results are shown in Table III.

Table III. Summary of the system performance with pole placement control

Time response characteristics	*Cart Position*	*Lower Pendulum angle*	*Upper Pendulum angle*
Ts (s)	0.0791	0.0487	0.1389
Ts (s)	1.6029	1.5413	1.7047
P.A (m/rad)	0.2249	0.1756	0.0893
e_{ss} (m/rad)	0	0	0

Where Tr is the rise time, Ts is the settling time, P.A is the peak amplitude and e_{ss} is the steady state error.

B. Simulation Results for Manual LQR Control

This subsection presents the simulation results (in Table IV) when the Q and R matrices were tuned manually, in a systematic way, to understand how the elements of the Q and R matrices contribute to the system response.

For each tuning case, the controller gain was calculated using this command in MATLAB: K_{lqr} = lqr (A, B, Q, R)

Table IV. Performance of DIP with manually tuned LQR

Q and R Matrices	*R. P*	*Results*		
		C.P	*L.P.A*	*U.P. A*
Q_1=diag (1, 1, 1, 1, 1, 1]) $R_1 = [1]$	**Tr (s)**	0.2854	0.2345	0.3532
	Ts (s)	4.9040	3.4513	3.5552
	P.A (rad)	0.4748	0.1053	0.0875
	e_{ss} **(rad)**	0	0	0
	J_lqr	0.0041		
Q_2=diag ([10000, 1, 1, 1, 1]) $R_2 = [1]$	**Tr (s)**	0.0764	0.0462	0.1379
	Ts (s)	1.5987	1.7343	2.0400
	P.A (rad)	0.2086	0.1800	0.0895
	e_{ss} **(rad)**	0	0	0
	J_lqr	10		
Q_3=diag ([10000, 1, 0.001, 1, 0.00 1,1]) $R_3 = [1]$	**Tr (s)**	0.0762	0.0448	0.1348
	Ts (s)	1.545	1.5887	1.7495
	P.A (rad)	0.2109	0.1799	0.0895
	e_{ss} **(rad)**	0	0	0
	J_lqr	4.0560		
Q_4=diag ([10000, 1, 1, 1, 1,1]) $R_4 = [0.01]$	**Tr (s)**	0.0554	0.0295	0.1102
	Ts (s)	1.3215	1.1461	1.5191
	P.A (rad)	0.1643	0.2680	0.0941
	e_{ss} **(rad)**	0	0	0
	J_lqr	8.8403		

Where R.P is the response parameters, C.P is the cart position, L.P.A is the lower pendulum angle and U.P.A is the upper pendulum angle.

Fig. 5, Fig. 6, and Fig. 7 show the response of the system when the matrices are set to Q_4 and R_4.

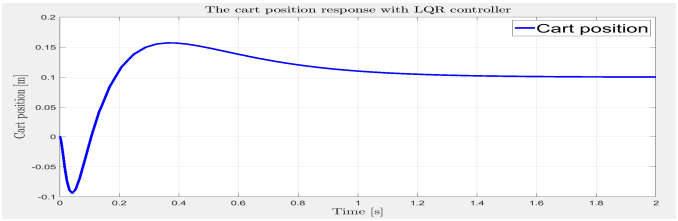

Fig. 5. The cart position response with LQR controller

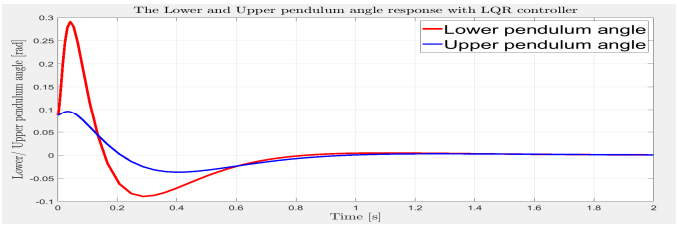

Fig. 6. The lower and upper pendulum angle response with LQR controller

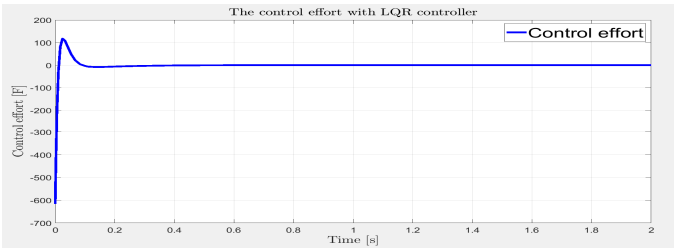

Fig. 7. The control effort with LQR controller

C. Simulation Results for GA and PSO Tunned LQR Control

Both optimizations were performed in MATLAB using GA and PSO toolboxes. And the summary of the results can be found in Table V.

Optimization parameters/ options: Initial population = 100; Maximum iterations/ Generations=3; Lower boundary, lb= [1 1 1 0.001]; Upper boundary, ub= [10000 10000 10000 10];

Table V. Performance of DIP with GA and PSO tuned LQR

Q and R Matrices	*R. P*	*Results*		
		C.P	*L.P.A*	*U.P. A*
GA Q= diag (1.0e+03 * [6.0587, 0.001, 3.5314, 0.001, 6.0716, 0.001]) $R = [0.034]$	**Tr (s)**	0.1367	0.0728	0.0440
	Ts(s)	2.332	1.9197	1.9109
	P.A (rad)	0.0901	0.1869	0.0901
	e_{ss} **(rad)**	0	0	0
	J_lqr	6.0587	**J_optim**	0.0047
PSO Q= diag (1.0e+04 *[1.0, 0.0001, 0.0001, 0.0001, 0.906, 0.0001]) $R = [0.001]$	**Tr(s)**	0.0564	0.0275	0.1077
	Ts(s)	1.4130	0.7512	1.0245
	P.A (rad)	0.1515	0.3094	0.0969
	e_{ss} **(rad)**	0	0	0
	J_lqr	3.7873	**J_optim**	0.0017

D. Animate the Dynamic Motion of DIP

To further validate the functionality of the designed controllers, an animation was created based on the numerical integration of the system non-linear ODE. Fig.8 shows some captured images while the animation was running.

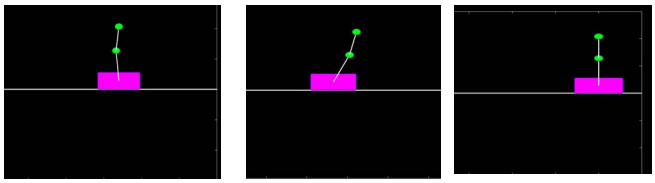

Fig. 8. 2D Animation of the system control

V. DISCUSSION

By examining the results in Table V and those in Table IV and III, it can be deduced that the PSO tuned LQR gave the overall best transient performance in comparison with the GA tuned and manually tuned LQR and the pole-placement controller. The settling time of the cart, the lower pendulum, and the upper pendulum were improved by 11.85%, 51.26% and 39.9% respectively by the PSO tuned LQR when compared with the results of the pole-placement controller. In addition, the results in Table V (in which similar optimization parameters were defined for GA and PSO) validates that PSO is better than GA when searching for the optimal values of the Q and R matrices used in LQR control.

VI. CONCLUSION

In this paper, the model of a double inverted pendulum was developed using Euler-Lagrange dynamic formulation, and pole placement and LQR controllers were designed to stabilize the system. The performance of each controller was tested in MATLAB/Simulink simulation environment and the system gave satisfactory results based on the control goals and requirements: the pendulums stabilized in less than 3 s with an overshoot less than 20 degrees and the cart move to 0.1 meters in less than 3 seconds with a rise time less than 0.5 s. Furthermore, the Q and R matrices of the LQR controller were tuned by using GA and PSO algorithms. From the simulation results, the PSO-tuned LQR controller gave the overall best transient performance in comparison with the GA tuned and manually tuned LQR and the pole-placement controller.

The future aspect of this research will be centred on the development of a modular and cheap double inverted pendulum system, including intelligent and robust control.

REFERENCES

[1] I. Siradjuddin, B. Setiawan, A. Fahmi, Z. Amalia, and E. Rohadi, "State space control using LQR method for a cart-inverted pendulum linearised model," vol. 17, no. 01, p. 9, 2017.

[2] A. Cerda-Lugo, A. Gonzalez, A. Cardenas, and D. Piovesan, "Experimental Estimation of a Second Order, Double Inverted Pendulum Parameters for the study of Human Balancing," in *2019 41st Annual International Conference of the IEEE Engineering in Medicine and Biology Society (EMBC)*, Berlin, Germany, Jul. 2019, pp. 4117–4120, doi: 10.1109/EMBC.2019.8857611.

[3] A. KAMIL and et al., "A comprehensive approach to double inverted pendulum modeling," 2019, doi: 10.24425/ACS.2019.130201.

[4] K. Srikanth and N. K. G V, "Stabilization At Upright Equilibrium Position of a Double Inverted Pendulum With Unconstrained Bat Optimization," *Int. J. Comput. Sci. Appl.*, vol. 5, no. 5, pp. 87–101, Oct. 2015, doi: 10.5121/ijcsa.2015.5508.

[5] R. Banerjee, N. Dey, U. Mondal, and B. Hazra, "Stabilization of Double Link Inverted Pendulum Using LQR," in *2018 International Conference on Current Trends towards Converging Technologies (ICCTCT)*, Coimbatore, Mar. 2018, pp. 1–6, doi: 10.1109/ICCTCT.2018.8550915.

[6] Q. Qian, D. Dongmei, L. Feng, and T. Yongchuan, "Stabilization of the double inverted pendulum based on discrete-time model predictive control," in *2011 IEEE International Conference on Automation and Logistics (ICAL)*, Chongqing, China, Aug. 2011, pp. 243–247, doi: 10.1109/ICAL.2011.6024721.

[7] A. Jain, D. Tayal, and N. Sehgal, "Control of Non-Linear Inverted Pendulum using Fuzzy Logic Controller," *Int. J. Comput. Appl.*, vol. 69, no. 27, pp. 7–11, May 2013, doi: 10.5120/12141-8278.

[8] A. N. K. Nasir, "Performance Comparison between Sliding Mode Control (SMC) and PD-PID Controllers for a Nonlinear Inverted Pendulum System," vol. 4, no. 10, p. 6, 2010.

[9] A. Jose, C. Augustine, S. M. Malola, and K. Chacko, "Performance Study of PID Controller and LQR Technique for Inverted Pendulum," *World J. Eng. Technol.*, vol. 03, no. 02, pp. 76–81, 2015, doi: 10.4236/wjet.2015.32008.

[10] G. A. Sultan and Z. K. Farej, "Design and Performance Analysis of LQR Controller for Stabilizing Double Inverted Pendulum System," *Circ. Comput. Sci.*, vol. 2, no. 9, pp. 1–5, Oct. 2017, doi: 10.22632/ccs-2017-252-45.

[11] D. T. Ratnayake and M. Parnichkun, "LQR-Based Stabilization and Position Control of a Mobile Double Inverted Pendulum," *IOP Conf. Ser. Mater. Sci. Eng.*, vol. 886, p. 012034, Jul. 2020, doi: 10.1088/1757-899X/886/1/012034.

[12] T. F. Tang, S. H. Chong, and K. K. Pang, "Stabilisation of a rotary inverted pendulum system with double-PID and LQR control: experimental verification," *Int. J. Automation and Control*, p. 16, 2020.

[13] A. I. Isa, M. F. Hamza, and M. Muhammad, "Hybrid Fuzzy Control of Nonlinear Inverted Pendulum System," p. 14, 2019.

[14] S. K. Yadav and M. N. Singh, "Optimal Control of Double Inverted Pendulum Using LQR Controller," vol. 2, no. 2, p. 5, 2012.

[15] T. T. Sarkar and L. Dewan, "Pole-placement, PID and genetic algorithm based stabilization of inverted pendulum," in *2017 8th International Conference on Computing, Communication and Networking Technologies (ICCCNT)*, Delhi, Jul. 2017, pp. 1–6, doi: 10.1109/ICCCNT.2017.8204047.

[16] A. A. Roshdy, L. Yu zheng, H. F. Mokbel, and W. Tongyu, "Stabilization of Real Inverted Pendulum Using Pole Separation Factor," presented at the 1st International Conference on Mechanical Engineering and Material Science), China, 2012, doi: 10.2991/mems.2012.107.

[17] E. Vinodh Kumar and J. Jerome, "Robust LQR Controller Design for Stabilizing and Trajectory Tracking of Inverted Pendulum," *Procedia Eng.*, vol. 64, pp. 169–178, 2013, doi: 10.1016/j.proeng.2013.09.088.

[18] S.-J. Huang, S.-S. Chen, and S.-C. Lin, "Design and Motion Control of a Two-Wheel Inverted Pendulum Robot," vol. 13, no. 3, p. 8, 2019.

[19] K. Hassani and W.-S. Lee, "Optimal Tuning of Linear Quadratic Regulators Using Quantum Particle Swarm Optimization," p. 8, 2014.

[20] L. Moysis, "Balancing a double inverted pendulum using optimal control and Laguerre functions," p. 10, 2016.

[21] A. Al-Mahturi and H. Wahid, "Optimal Tuning of Linear Quadratic Regulator Controller Using a Particle Swarm Optimization for Two-Rotor Aerodynamical System," *Int. J. Electron. Commun. Eng.*, vol. 11, no. 2, p. 7, 2017.

[22] C. Sravan Bharadwaj, T. Sudhakar Babu, and N. Rajasekar, "Tuning PID Controller for Inverted Pendulum Using Genetic Algorithm," in *Advances in Systems, Control and Automation*, vol. 442, A. Konkani, R. Bera, and S. Paul, Eds. Singapore: Springer Singapore, 2018, pp. 395–404.

[23] M. A. Sen and M. Kalyoncu, "Optimal Tuning of a LQR Controller for an Inverted Pendulum Using the Bees Algorithm," *J. Autom. Control Eng.*, vol. 4, no. 5, p. 4, 2016.

[24] H. G. Kamil, O. T. Makki, and H. M. Umran, "Optimal tuning of a Linear Quadratic Regulator for Position Control using Particle Swarm Optimisation," *IOP Conf. Ser. Mater. Sci. Eng.*, vol. 671, p. 012047, Jan. 2020, doi: 10.1088/1757-899X/671/1/012047.

[25] Hazem I. Ali and Alza A. Mahmood, "LQR Design using Particle Swarm Optimization.pdf." Iraq Academic Scientific Journals, 2016, [Online]. Available: https://www.iasj.net.